Fuel 324 (2022) 124677

Contents lists available at ScienceDirect

Fuel

journal homepage: www.elsevier.com/locate/fuel

Full Length Article

Multi-scale modelling of fluidized bed biomass gasification using a 1D particle model coupled to CFD

Lukas von Berg [a,*], Andrés Anca-Couce [a,b], Christoph Hochenauer [a,c], Robert Scharler [a,c]

[a] Graz University of Technology, Institute of Thermal Engineering. Inffeldgasse 25/B, 8010 Graz, Austria
[b] Carlos III University of Madrid, Thermal and Fluids Engineering Department, Avda. de la Universidad 30, 28911 Leganés, Madrid, Spain
[c] BEST – Bioenergy and Sustainable Technologies GmbH, Inffeldgasse 21b, 8010 Graz, Austria

ARTICLE INFO

Keywords:
Multi-scale modelling
Particle model
CFD
Fluidized bed
Biomass
Gasification

ABSTRACT

For many fluidized bed applications, the particle movement inside the reactor is accompanied by reactions at the particle scale. The current study presents for the first time in literature a multi-scale modelling approach coupling a one-dimensional volumetric particle model with the dense discrete phase model (DDPM) of ANSYS Fluent via user defined functions. To validate the developed modelling approach, the current study uses experimental data of pressure drop, temperature and gas composition obtained with a lab-scale bubbling fluidized bed biomass gasifier. Therefore, a particle model developed previously for pyrolysis was modified implementing a heat transfer model valid for fluidized bed conditions as well as kinetics for char gasification taken from literature. The kinetic theory of granular flow is used to describe particle–particle interactions allowing for feasible calculation times at the reactor level whereas an optimized solver is employed to guarantee a fast solution at the particle level. A newly developed initialization routine uses an initial bed of reacting particles at different states of conversion calculated previously with a standalone version of the particle model. This allows to start the simulation at conditions very close to stable operation of the reactor. A coupled multi-scale simulation of over 30 s of process time employing 300.000 inert bed parcels and about 25.000 reacting fuel parcels showed good agreement with experimental data at a feasible calculation time. Furthermore, the developed approach allows for an in-depth analysis of the processes inside the reactor allowing to track individual reacting particles while resolving gradients inside the particle.

1. Introduction

According to the Intergovernmental Panel on Climate Change [1], drastic reductions in CO_2 and other greenhouse gas emissions are required to limit the effects of human-induced global warming. Biomass can be considered a CO_2-neutral source of energy when harvested sustainably and therefore plays a key role in substituting fossil fuels to achieve a reduction of greenhouse gases [2]. Whereas biomass combustion is already a mature technology and widely used, gasification of biomass is a promising thermochemical conversion route which needs further development to reach full commercial status. Biomass gasification allows to produce a valuable gas which can be deployed in several applications like gas turbines or solid oxide fuel cells to generate power or to produce biofuels and chemicals [3].

Different reactor concepts for biomass gasification were developed in the past, whereas facilities based on the fluidized bed technology showed to be very promising. Fluidized bed reactors show advantageous characteristics due to the high thermal inertia of the bed, proper heat and mass transfer rates as well as adequate mixing rates and further allow easier scale-up of the process when compared to other reactor concepts [4]. However, further development of the concept of fluidized bed biomass gasification is still necessary in order to achieve high char conversion rates and to minimize the amount of tar contaminants in the gas which can hinder its application due to tar condensation in downstream facilities. As measurements are expensive and sometimes difficult due to limited accessibility, numerical modelling methods are a common tool used for the development and optimization of fluidized bed reactors. To achieve an accurate description of the process, different scales need to be considered. On the one hand, the movement of particles at the reactor level needs to be described sufficiently accurate in order to account for the dynamics of the bed. On the other hand, the conversion of the fuel at the particle level needs to be resolved. The aim of this study is to develop a CFD-based multi-scale approach combining a

* Corresponding author.
E-mail address: lukas.vonberg@tugraz.at (L. von Berg).

https://doi.org/10.1016/j.fuel.2022.124677
Received 30 March 2022; Received in revised form 16 May 2022; Accepted 22 May 2022
Available online 7 June 2022

Nomenclature

Abbreviations

BW-WGS	Backward water gas shift
CFD	Computational fluid dynamics
CV	Control volume
DDPM	Dense discrete phase model
DEM	Discrete element method
FBBG	Fluidized bed biomass gasification
FW-WGS	Forward water gas shift
HTM	Heat transfer model
KTGF	Kinetic theory of granular flow
MFC	Mass flow controller
MP-PIC	Multiphase particle-in-cell
ODE	Ordinary differential equation
PM	Particle model
SR	Steam reformation
TC	Tar cracking
TFM	Two-fluid model

model for the particle movement with a detailed model describing the conversion at the particle level while considering intra-particle gradients. In the current study, the developed modelling approach will be validated using representative experimental data of biomass gasification in a bubbling fluidized bed. However, the developed modelling approach can be applied not only to fluidized bed gasification of biomass, but can be used with specific adaptations for various biomass conversion plants based on fluidized bed technology and is therefore a very versatile tool for the development of such reactors.

1.1. Modelling strategies employed in literature

A comprehensive review about modelling biomass gasification in a fluidized bed is given by Gómez-Barea and Leckner [5]. They evaluated different modelling approaches and state that the so-called fluidization model, which approximates the reactor fluid dynamics based on semi-empirical correlations, was the best developed model at the time their study was released. A more basic approach using a black box model consists of overall balances (e.g., heat and mass) over the reactor and often assumes chemical equilibrium. As such a model does not resolve fluid dynamics and dispenses detailed kinetics, its prediction capability is not as good as for the other approaches. Finally, they conclude that models based on computational fluid dynamics (CFD) are still very time consuming and rely on various sub-models while not leading to a huge improvement compared to a fluidization model as modeling of the source terms is not more precise. However, they stress that the main advantage of Lagrangian-based CFD models, which allow for an easy consideration of particle size distributions and makes it possible to track the changes in physico-chemical characteristics of the biomass particles during conversion along their path through the reactor, is not yet been deployed by researchers. CFD models have been used more and more in recent years by researchers for fluidized bed modelling as computing power increases constantly allowing for feasible calculation times. The different CFD approaches are evaluated in the following paragraph.

At the reactor level, there are several CFD modelling strategies commonly employed for fluidized bed reactors which can generally be divided whether they are based on the Euler-Euler or the Euler-Lagrange approach [6]. The two-fluid model (TFM) considers both the gaseous as well as the particulate phase as two interpenetrating continua based on the Euler approach. Particle-particle interactions can be considered based on the framework of the kinetic theory of granular flow (KTGF) presented by Ding and Gidaspow [7]. Interaction of granular and continuous phase is considered via momentum exchange terms which are based on drag models. This approach is frequently used to model fluidized bed reactors [5]. The main disadvantage of this model is the high computational demand if a broad range of particle sizes needs to be considered as each particle size demands an additional phase. Furthermore, this method does not allow to track the movement and conversion of individual particles which makes it impossible to exploit the main advantage of CFD modelling of fluidized bed reactors. The other common approach to model fluidized bed reactors is based on the Euler-Lagrangian framework, which tracks individual particles by means of Newtons 2nd law of motion while the continuous phase is treated using the Eulerian description. For the Euler-Lagrangian approach, there are different ways in which particle–particle and particle–wall interaction are treated. The discrete element method (CFD-DEM) first introduced by Cundall and Strack [8] predicts collisions based on a soft-sphere approach, which leads to a realistic description of particle movement due to the detailed modelling of the collisions. However, extremely small time-steps are necessary which makes this approach very computationally demanding hindering its application for industrial-scale facilities [6]. Therefore, models based on the multiphase particle-in-cell (MP-PIC) approach [9,10] as the dense discrete phase model (DDPM) in ANSYS Fluent [11] were derived using a simplified way to approximate particle–particle interactions. Thereby, particle properties calculated based on the Lagrangian description are interpolated to the Eulerian grid used to describe the fluid flow which allows to employ the KTGF to consider collisions in an efficient way. Furthermore, this approach allows to cluster a group of particles in so called parcels to further reduce the computational demand. Although these hybrid approaches have a shorter history compared to other CFD approaches, they have been investigated intensively recently [12]. The cold-flow modelling study by Cloete et al. [13] investigating fluid-dynamics in a bubbling fluidized bed reactor showed that the DDPM is well suited for such applications. Furthermore, the study of Adnan et al. [14] presents an in depth investigation using the DDPM to describe the hydrodynamic behavior of a pilot-scale bubbling bed reactor. They investigated the effects of drag force, grid size, fluid time-step, time-averaging interval, particle–wall specularity coefficient, particle–particle restitution coefficient, particle–wall reflection coefficient and numbers of parcels [14]. They validated the model with experimental data and conclude that it is able to accurately reproduce the hydrodynamics of a bubbling fluidized bed. Furthermore, a study by Schneiderbauer et al. [15] showed the applicabillty of the DDPM in combination with an unreacted shrinking core model for the simulation of iron ore reducion in industrial-scale fluidized beds.

A comparison of modelling results for biomass gasification in a fluidized bed employing the MP-PIC model and the CFD-DEM is given by Li and Eri [16]. They conclude that the MP-PIC model (which is quite similar to the DDPM), despite showing some discrepancies on the particle scale when compared to the CFD-DEM results, is well suited to model reactor-scale applications. A comparison of the TFM and DDPM by Adnan et al. [14] showed similar results for the fluid dynamics of a lab-scale fluidized bed, whereas better grid independency was found for the DDPM making it a suitable choice for large-scale applications where coarse grids are needed. Overall, the DDPM and similar models based on the MP-PIC approach are getting more popular as they show significant advantages compared to TFM and CFD-DEM especially when modelling industrial scale applications.

A summary of literature dealing with modelling of fluidized bed biomass gasification (FBBG) employing CFD is given by Ostermeier et al. [17] (including papers published between 2014 and 2019). When analyzing these 19 publications, it can be seen that researchers employed 2D and 3D geometries in equal shares. The three main modelling approaches all showed a high relevance but the TFM (42%) was still the most favored one compared to MP-PIC/DDPM (32%) and CFD-DEM (26%). The analysis of more recent studies investigating CFD modelling of FBBG [17-21] (including papers published between 2019 and 2022) shows a very strong trend towards the Euler-Lagrange

approach. None of these recent studies employ the TFM approach whereas the MP-PIC/DDPM and the CFD-DEM are applied equally often. All these studies use 3D geometries. However, the particle scale of all these studies is modelled using a simplified zero-dimensional model and commonly employ single-step global reaction mechanisms. Therefore, models presented in current literature can only describe particle conversion with severe simplifications.

1.2. Importance of the particle-scale modelling

When looking at the particle level, drying, devolatilization and gasification of a biomass particle leads to the release of gases which has to be considered as source terms when modeling the fluid dynamics at reactor scale. Furthermore, energy source terms, e.g. for the endothermic gasification reactions, need to be calculated and coupled with the model at the reactor level. Therefore, models for biomass drying and devolatilization as well as char gasification need to be considered. Dimensionless numbers illustrate which processes dominate the conversion and indicate if simplifications can be made when developing a model. A detailed investigation can be found in Gomez-Barea and Leckner [5]. The Biot number Bi, defined as the ratio of the thermal resistance inside a particle and at the surface of a particle, is an indicator if particle-internal temperature gradients are present. An analog consideration leads to the mass transfer Biot number Bi_m, which indicates the presence of species gradients inside a particle. If the Biot number is either very small or very high, one of the processes (external or internal, respectively) is dominating which allows to simplify the modelling procedure. However, for intermediate values, internal gradients are relevant and both external and internal processes must be considered. As shown by von Berg et al. [23], the Biot number for typical biomass particles inside a fluidized bed is in the intermediate range which indicates the requirement of a spatial resolution of the particle as well as a sophisticated heat transfer model. The study of Dupont et al. [24] also concludes that for particles>0.1 mm, external heat transfer and conduction inside the particle are on the same time scale and that pyrolysis (at gasification conditions) is controlled by both heat transfer and chemical kinetics. They state that gasification is controlled mainly by chemical kinetics assuming it occurs uniformly over the whole particle independently of particle size. However, studies of Mermoud et al. [25] and Van de Steene et al. [26] show the relevance of particle size on the conversion time based on experimental data and single particle modelling. Bates et al. [27] conducted a time scale analysis of biomass particles in a fluidized bed environment and state that heat transfer limitations dominate pyrolysis and drying as these processes show rather fast kinetics. They found a Biot number close to 1 for 6 mm particles which means internal temperature gradients are present. Further, they state that for particles between 0.5 and 6 mm, which are typical for fluidized bed applications, mixing and heat transfer are happening simultaneously.

Therefore, a detailed particle model is necessary for an adequate description of the conversion of the reacting particle. Sophisticated particle models are usually employed for single particle analysis. However, such detailed approaches are commonly not employed combined with a reactor model as the huge number of particles makes it very time consuming. To the best knowledge of the authors, there is no study in literature which describes the particle conversion in FBBG using a one-dimensional model able to describe gradients inside the particle coupled with a CFD description of the reactor level. Such a coupled approach, however, would allow for a more realistic description of the physical processes compared to state-of-the-art literature. A review by Baruah and Baruah [28] states the importance of a model combining a detailed description of the chemical phenomena with an accurate description of multiphase flow. Furthermore, the recent review of biomass gasification modelling by Safarian et al. [29] emphasizes the importance of comprehensive models especially in the case of fluidized bed reactors, where detailed kinetics need to be combined with accurate fluid dynamic modelling. In the recently published review paper of Alobaid et al. [12] about CFD simulations of fluidized bed reactors, the importance of studies combining a detailed description of the gas flow and the particle movement as well as the heterogeneous reactions while considering intra-particle gradients is furthermore emphasized for future work. However, detailed particle models resolving gradients inside the particle are usually very computationally demanding. Especially the fact that the boundary conditions of the particles change constantly as they move through the bed makes it furthermore challenging. Therefore, Anca-Couce and Zobel [30] developed a single particle model based on an iterative fractional-step algorithm especially optimized to be coupled to a Lagrangian reactor model. Their approach showed to be significantly faster compared to other solving strategies when changing boundary conditions need to be considered.

In the present study, a detailed particle model (PM) developed for biomass conversion by Anca-Couce and Zobel [30] was adapted and coupled with the dense discrete phase model (DDPM) implemented in the commercial CFD software ANSYS Fluent via user defined functions. The PM used is based on a solver optimized for fast solution under constantly changing boundary conditions. This allows for a comprehensive description of the conversion process of biomass in a fluidized bed gasifier considering a detailed description at the reactor scale as well at the particle scale. The model is validated with experimental results obtained with a steam blown lab-scale bubbling fluidized bed biomass gasifier in the framework of this study. Furthermore, the newly developed modelling approach can also be employed for many different fluidized bed applications with rather small adaptions when a detailed description of the particle level is of importance like e.g. for fluidized bed combustion or chemical looping.

2. Numerical modelling

The modelling approach is based on a one-dimensional particle model which describes the conversion process of the fuel particle including heat-up, drying, devolatilization and char gasification while considering gradients in the particle. This particle model is coupled to the DDPM implemented in the commercial CFD software (ANSYS Fluent V2021 R2) used to describe the gaseous and solid phase at the reactor level. The following section gives an overview of the employed models.

2.1. Reactor level

A CFD model able to track individual particles is necessary to implement the coupled modelling approach to be able to describe the conversion of reacting particles along their trajectory through the reactor. The TFM does not track individual particles and can therefore not be directly employed. The discrete phase model (DPM) is a Euler-Lagrange model implemented in ANSYS Fluent and allows to track individual particles. It is based on the assumption that the volume fraction of the particle phase is very small which is therefore not considered in the continuity and momentum equations of the continuous phase. However, when high particle loadings as in a fluidized bed reactor are present, this assumption is not valid. Therefore, the reactor level is modelled using the framework of the dense discrete phase model (DDPM) based on a hybrid Euler-Lagrange approach suitable at higher particulate loadings. In addition, the DDPM allows to introduce source terms due to the heterogeneous reactions calculated by the particle model into the mass and energy equations of the gas phase. This is particularly important as the additional gas flow affects the particle motion predicted by the DDPM. The basic theory of the DDPM and a description of the kinetic theory of granular flow (KTGF) used to model particle collisions as well as the employed sub-models can be found in the supplementary material. The drag model of Gidaspow [31] recommended for dense fluidized beds [11] was employed, a discussion of different drag models including the more recently employed filtered models is given in the supplementary material. A comprehensive pre-

study was conducted in the framework of this work to investigate the applicability of the DDPM for bubbling fluidized bed reactors. The results are presented in the master thesis of Blehrmühlhuber [32] supervised by two of the authors of the current study. In general, good agreement of experimental data provided by the NETL [33] and modelling results (pressure-drop, particle velocities, general patterns of particle movement) was found. This pre-study was the foundation for the fluid-dynamic modelling for the current manuscript. A summary of the employed models and sub-models of the DDPM and the KTGF in the present study can be found in section 3.2. It has to be mentioned that radiation was not considered at the reactor scale for the sake of simplicity whereas it is included for the reacting particles. This simplification is supported by the high optical thickness of the particle bed, which means that the inert bed particles are only in radiation exchange with their immediate surroundings which show very similar temperature due to the homogenous temperature distribution inside a fluidized bed. However, a radiation model at the reactor level should be used in future studies.

2.1.1. Limitations of the DDPM

The DDPM is frequently used for fluidized bed modelling, however, there are some limitations that can lead to difficulties in the application of the model. Pre-tests conducted in this study showed that the description of the particulate phase was not working at a gas velocity lower than the minimal fluidization velocity when the KTGF is used to model particle collisions in the framework of the DDPM. In this case we would expect the particles to form a fixed bed. However, the model showed a completely unrealistic particle behaviour, with all particles accumulating and overlapping in a single layer at the very bottom. Furthermore, the pressure drop cannot be described realistically in this case. Similar behaviour is also described by Tricomi et al. [34]. This limitation might lead to problems when modelling full-scale dual fluidized bed facilities where regions showing low fluidization can be present e.g. in the loop seals connecting the two reactors.

Furthermore, the ratio of the cell size to the parcel size needs to be considered carefully when using the DDPM [35]. Values obtained from the Lagrangian solution need to be averaged for each cell before they can be used in the Eulerian framework. Therefore, it is important that the cells are big enough for a sufficient number of particles. Otherwise, averaging can lead to distorted values [32] and furthermore, numerical instabilities can arise e.g. in the case when the whole volume of a cell is occupied by a single parcel [17]. Usually coarse meshes are employed when using a hybrid Euler-Lagrange approach to fulfil the before mentioned limitation. However, a compromise has to be found to achieve a mesh that can resolve fine scale structures but is still large enough to ensure a cell size sufficiently larger than the parcel size. When the cell size cannot be further increased but the particles are still too big to fulfil this limitation, the DDPM provides the possibility to employ a reverse clustering (i.e. splitting) approach where one particle is represented by several smaller computational parcels. The number of parcels employed in the current study to represent the bed material and fuel particles is further discussed in section 3.3. The problem of parcel-to-cell ratio is further discussed by Yang et al. [36]. They suggest a method to overcome numerical instabilities when parcels cross small cells by implementing a distribution kernel method (DKM) spreading solid volume and source terms of parcels to the domain in which the particles are clustered.

2.1.2. Homogeneous reactions

Homogeneous gas phase reactions consider water gas shift, methane steam reformation and tar cracking and are modelled using the finite rate/eddy dissipation model of Fluent [37]. The employed reaction mechanisms and kinetics are summarized in Table 1.

The tar content in the gas produced during biomass gasification is essential as it is one of the main obstacles regarding the application of the gas. High tar loadings lead to fouling and can damage down-stream facilities. However, a detailed description of tar kinetics is very complex which is why most FBBG simulations in literature employ a rather simple tar cracking mechanism despite its importance. In the current study, the stoichiometry of the tar cracking reaction was estimated based on a detailed pyrolysis reaction scheme in a similar way as in the study of Scharler et al. [41] employing a lumped tar species. A standalone simulation of the particle model employing detailed pyrolysis kinetics was used to determine the gas composition considering 16 tar species similar as shown in the study of Anca-Couce et al. [42]. The products of the lumped tar cracking reaction were calculated based on a modified version of the detailed thermal tar cracking reactions proposed by Mellin et al. [43] considering H_2, CO, CO_2, CH_4 and C_6H_6 in the gas composition. In comparison to Mellin et al. [43], solid carbon and C_2H_4 (which is included in the CH_4 yield) were not considered in the current study, whereas C_6H_6 was considered in this work and not by Mellin et al.. All the tar components of the detailed scheme were lumped into one tar species considering C, H and O in the elemental composition. A reaction mechanism based on a simple one-step reaction as shown in reaction (R4) was employed to consider tar cracking as a homogeneous gas phase reaction. Although simplified, the current approach is based on a detailed mechanism with multiple species and therefore allows to increase the complexity of tar modelling with manageable effort for future applications e.g. by implementing additional tar species released from the particle model and additional tar cracking reactions in the gas phase respectively.

2.2. Particle level

The particle level is based on the one-dimensional model developed for biomass pyrolysis by Anca-Couce and Zobel [30]. They compared different solution methods for solving a single particle model and investigated their potential for coupling with a Euler-Lagrange reactor model. The main difficulties in this case are the boundary conditions, which change constantly as the particle is moving through the reactor. This is especially time consuming in the case of ODE solvers commonly used for single particle modelling. As such models show a high computationally demand for initialization, they are not well suited for the coupling into a reactor model as initialization is necessary at each time-step. The time-step of reactor models for fluidized beds is in the range of milliseconds which, together with the huge number of particles,

Table 1
Homogeneous gas phase reactions (values in square brackets have units of kmol/m^3).

	Reaction	Reaction rate r in kmol / (m^3·s)	
Forward water gas shift [38]	$CO + H_2O \rightarrow CO_2 + H_2$	$r_{FW-WGS} = 2.78 \bullet 10^3 \bullet \exp\left(\frac{1.26 \bullet 10^7}{RT}\right)[CO][H_2O]$	(R1)
Backward water gas shift [38]	$CO_2 + H_2 \rightarrow CO + H_2O$	$r_{BW-WGS} = 9.59 \bullet 10^4 \bullet \exp\left(\frac{4.66 \bullet 10^7}{RT}\right)[CO_2][H_2]$	(R2)
Steam reformation [39]	$CH_4 + H_2O \rightarrow CO + 3\ H_2$	$r_{SR} = 5.92 \bullet 10^8 \bullet \exp\left(\frac{2.09 \bullet 10^8}{RT}\right)[CH_4]^{0.5}[H_2O]$	(R3)
Tar cracking [40]	$Tar \rightarrow 0.707\ H_2 + 1.054\ CO + 0.219\ CO_2 + 0.489\ CH_4 + 0.103\ C_6H_6$	$r_{TC} = 3.7 \bullet 10^7 \bullet \exp\left(\frac{1.19 \bullet 10^8}{RT}\right)[Tar]$	(R4)

is the main driver of high computation times. Therefore, they developed a model based on an iterative fractional step algorithm which showed to be the fastest approach and will be used further on in this study. This approach allows to solve different phenomena either in an explicit, implicit or semi-implicit way according to their characteristic times and to use advantageous solving strategies for each phenomenon when applicable. A detailed description of the solving procedure can be found in [30]. In the current work, the particle model was adapted to be able to describe gasification of spherical or cylindrical softwood pellets in a fluidized bed reactor.

The particle is discretized using several control volumes (CV). Transport of mass inside the particle is considered via convection and diffusion whereas heat transfer is considered via conduction and convection. Diffusion is modeled via Fick's law whereas the diffusion coefficients of the different species are calculated based on the Chapman-Enskog equation (assumption of diffusion of each species in nitrogen). Shrinkage of the particle is considered during pyrolysis and gasification for each individual CV according to the local conversion. A standalone version of the model was programmed in C, which later on allowed for easy implementation as a user-defined function in Fluent for the coupled model. The adapted version of the model considers drying, pyrolysis and gasification with H_2O and CO_2 of the biomass particle summarized in Table 2.

Drying is modelled following reaction (R5) with a first-order Arrhenius equation [44]. Pyrolysis is described via a single-step global reaction scheme shown in (R6) whereas the reaction rate was calculated using kinetics given in literature [44]. The stoichiometric factors of the pyrolysis products were approximated based on the results of the detailed single particle model developed by Anca-Couce et al. [42] employing a comprehensive pyrolysis mechanism based on the mechanism of Ranzi et al. [45]. A single particle simulation using the detailed model was conducted once employing boundary conditions representative for the investigated case and the results were used to calculate the composition of permanent gases, a lumped species representing tar components as well as the amount of char residue. This allows for a detailed description of pyrolysis while using a time-saving reaction mechanism. As the currently employed simplified pyrolysis model is based on a detailed model, a further increase in complexity can be easily implemented if required, e.g. by considering additional tar species. The composition of char is derived from the detailed model considering not only pure carbon but also hydrogen (α_C) and oxygen (β_C) in the char. Gasification of the residual char is regarded by H_2O (R7) and CO_2 (R8) whereas the composition of char is respected. The kinetics of CO_2 gasification by Van de Steene et al. [26] were employed. Two different kinetics for H_2O gasification by Mermoud et al. [25] and Van de Steene et al. [26] were investigated. As shown later on (see section 4.1.1), the kinetics of Van de Steene et al. seemed to be better suited and were therefore employed in the following simulations.

Boundary conditions of the particle model need to be chosen carefully and adaptations to the original particle model were necessary to respect conditions in a fluidized bed. In a previous study by von Berg et al. [23], different correlations modelling the heat transfer to a biomass particle submerged in a fluidized bed were implemented to a single particle model. The objective of that study was to gain a comprehensive understanding of heat transfer phenomena in the case of fuel particles in a fluidized bed and to provide the foundation for the heat transfer modelling used in our present work. Validation showed reasonable agreement of modelling results for all heat transfer models when compared to experimental data of biomass pyrolysis conducted in a fluidized bed at high gas velocities when using softwood pellets as fuel. However, models like the one of Agarwal [46], which include the effect of fluidization velocity, are more versatile and valid for a broader range of operation conditions. It was found that especially in cases of very low fluidization velocities, deviations with experimental data are present. Therefore, the model of Agarwal [46] was chosen. The model of Agarwal considers a particle convective component, a gas convective component while the particle is in the emulsion phase and a gas convective component while being in the bubble phase. Radiation is not considered. These contributions are weighted using probabilities to calculate the heat transfer coefficient to a single particle. Due to the complexity of the model, it is not further described here and the reader is referred to reference [46] for more information. To respect mass transfer to a particle in a fluidized bed, the Sherwood number used to determine the mass transfer coefficient was calculated as $Sh = 2\varepsilon + 0.69(Re_p/\varepsilon)^{1/2}Sc^{1/3}$ as given in [47]. Temperature, gas composition and gas velocity have to be set to a constant value for standalone calculations. In the coupled model, these boundary values will be taken from the cell in which each particle resides. The heat transfer coefficient calculated via the model of Agarwal based on the conditions in the CFD-cell as well as the gas temperature of the CFD-cell are used in an energy balance at the surface of the reacting particle to calculate the surface temperature. In this balance, radiation from the surrounding inert bed to the fuel particle is considered assuming that the particle bed has a high optical thickness. Further on, this surface temperature is then used in the energy balance at the outermost control volume. In a similar way, the mass transfer coefficient calculated based on the Sherwood number and the gas composition of the CFD-cell are employed in the mass balance of the outermost control volume of the particle. The most important parameters for the particle model as well as values which determine the initial condition of a biomass particle are presented in Table 3.

Table 3
Important model parameters of the particle model and initial conditions.

Model parameters:		
Thermal conductivity biomass	0.177	W/(m • K)
Thermal conductivity char	0.1	W/(m • K)
Solid density	1500	kg/m^3
Minimum shrinkage factor	0.46	–
Heat capacity biomass	$1500 + T$	J/(kg • K)
Heat capacity char	$420 + 2.09 \bullet T - 6.85 \bullet 10^{-4} \bullet T^2$	J/(kg • K)
Heat capacity water	4200	J/(kg • K)
Permeability biomass	$1 \bullet 10^{-14}$	m^2
Permeability char	$1 \bullet 10^{-12}$	m^2
Pore diameter	$1 \bullet 10^{-4}$	m
Emissivity	0.9	–
Dynamic viscosity gas	$1 \bullet 10^{-5}$	kg/(m • s)
Thermal conductivity gas	0.0258	W/(m • K)
Initial conditions (fresh biomass):		
Initial porosity	19.13	%
Particle radius	0.003	m
Particle length	0.018	m
Moisture	8	%
Initial biomass density (wet)	1319	kg/m^3
Initial temperature	300	K

Table 2
Heterogeneous reactions (values in square brackets have units of kg/m^3).

	Reaction	Reaction rate r in kg / (m^3·s)	
Drying [44]	$H_2O\ (l) \rightarrow H_2O\ (g)$	$r_{drying} = 5.56 \bullet 10^6 \bullet e^{-87.9kJ/(R \bullet T_{CV})}[H_2O]_{CV}$	(R5)
Pyrolysis [44]	$Biomass\ (s) \rightarrow Char\ (s) + CO + H_2O + CO_2 + H_2 + CH_4 + Tar$	$r_{pyrolysis} = 2.0 \bullet 10^8 \bullet e^{-133.1 \bullet 10^3/(R \bullet T_{CV})}[Biomass]_{CV}$	(R6)
CO_2 gasification [26]	$Char\ (s) + CO_2 \rightarrow 2\ CO + \left(\frac{\alpha_C}{2} - \beta_C\right) H_2 + \beta_C\ H_2O + Ash\ (s)$	See reference	(R7)
H_2O gasification [26]	$Char\ (s) + (1 - \beta_C)\ H_2O \rightarrow CO + (1 + \alpha_C/2 - \beta_C)\ H_2 + Ash\ (s)$	See reference	(R8)

The number of grid points resolving the particle can be chosen individually. For the current study, a number of 10 control volumes (CV) along the particle radius showed virtually grid-independent resolution of intra-particle gradients while keeping the calculation demand low. A further refinement did not improve the results significantly, but could be necessary when modelling larger particles.

During the conversion of a fuel particle in the reactor it is exposed to thermal and mechanical stresses which can cause the particle to break into several small pieces. This process is called primary fragmentation. During the subsequent conversion of the char, the particle fragments suffer from further decay due to increasing pores and a decreasing stability of the char structure, called secondary fragmentation. Furthermore, attrition of the fuel leads to the formation of fine particles due to the abrasive effects caused by the intensive contact of fuel particles with the bed material. General modelling approaches for this phenomenon can be found in [5]. A transient particle model for the conversion of biomass char in a fluidized bed gasifier considering fragmentation and attrition was presented by Bates et al. [48]. As this process is very complex and furthermore depends on the properties of the employed biomass type, fragmentation is usually not modelled in CFD studies and is also not considered in this study.

2.3. Coupling of reactor and particle level

The particle model was adapted to be able to describe gasification of biomass particles in a fluidized bed environment (see chapter 2.2). This model needs to be coupled to a CFD code (see chapter 2.1) which allows to describe the fluid dynamics of the bed and the gas phase reactions.

The PM provides results at the particle level and is implemented into ANSYS Fluent using so called user-defined functions (UDF) in C–programming language. The reactor level is described using the DDPM implemented in Fluent. A basic scheme of the coupling approach including the employed sub-models is depicted in Fig. 1. At the particle level, the temperature, gas composition and gas velocity are taken from the current cell at the reactor level and are used as boundary condition for the particle model. The particle model is solved for each biomass particle at every time-step of the CFD model. Source terms for gas species and energy are calculated and forwarded to Fluent where they are considered in the conservation equations of the gaseous phase. The results of the PM necessary for the calculation of the PM at the next time-step are stored in so-called particle user-variables for every particle. Furthermore, the solution for temperature, density, mass and diameter calculated by the PM are written to each corresponding particle in the reactor model. When employing a cylindrical shape in the particle model, the diameter of the mass equivalent sphere is used for the reactor model as only spheres are supported in the DDPM.

The concept presented above can also be applied when particles are clustered in parcels. This is commonly done when a huge number of particles is present in order to reduce computational cost. In this case, the PM gets solved for each parcel, however, the real diameter, mass, etc. of the actual particle is used for the solution of the PM. The source terms must then be corrected with the number of particles per parcel.

3. Experimental rig and simulation setup

The model developed in this study is validated using experimental data of a steam blown lab-scale fluidized bed biomass gasifier. The following section describes the experimental rig prior to a detailed description of the simulation setup and the boundary conditions.

3.1. Experimental setup

A scheme of the experimental rig is shown in Fig. 2 on the left. Preheated steam at 673 K is led to the reactor from the bottom. About 900 g of olivine with a mean diameter of 260 μm and a particle density of 2965 kg/m^3 was used as bed material. The experiments were conducted using softwood pellets as fuel with a cylindrical shape, a diameter of 6 mm and an average length of 18 mm. Several thermocouples along the height of the reactor as well as a differential pressure sensor to measure the pressure drop over the bed are installed to monitor the process. The average operating temperature is kept at a constant level of 1073 K via an electric heating whereas the mean value of T_1, T_2 and T_3 is used to regulate the electric heating. The fuel is fed to the fluidized bed from the top using a screw feeder. A nitrogen flow of 0.13 kg/h is led through the pellets tank to achieve an inert atmosphere and to prevent that moist syngas can reach the fuel tank. The bed is fluidized using a mixture of 0.42 kg/h of steam and 0.02 kg/h nitrogen via a nozzle in the center of the reactor. The steam flow is distributed radially across the reactor cross-section via a nozzle with 6 orifices. The pressure drop of the distributor with the employed settings is comparably small showing about 40 Pa, however, as the nozzle is located in the center of the reactor, we can assume a constant steam-feed in this position. This setup does not allow for a perfectly evenly distributed gas flow over the cross-section of the reactor and small dead-spots in the bottom-corner can be expected. The syngas leaves the gasifier at the top and is cleaned in a candle filter to remove particulate matter. A pressure regulator keeps the pressure in the system at 0.5 bar. After the gas leaves the facility, a part of it is further cleaned to remove tars and the permanent gases CO, CO_2,

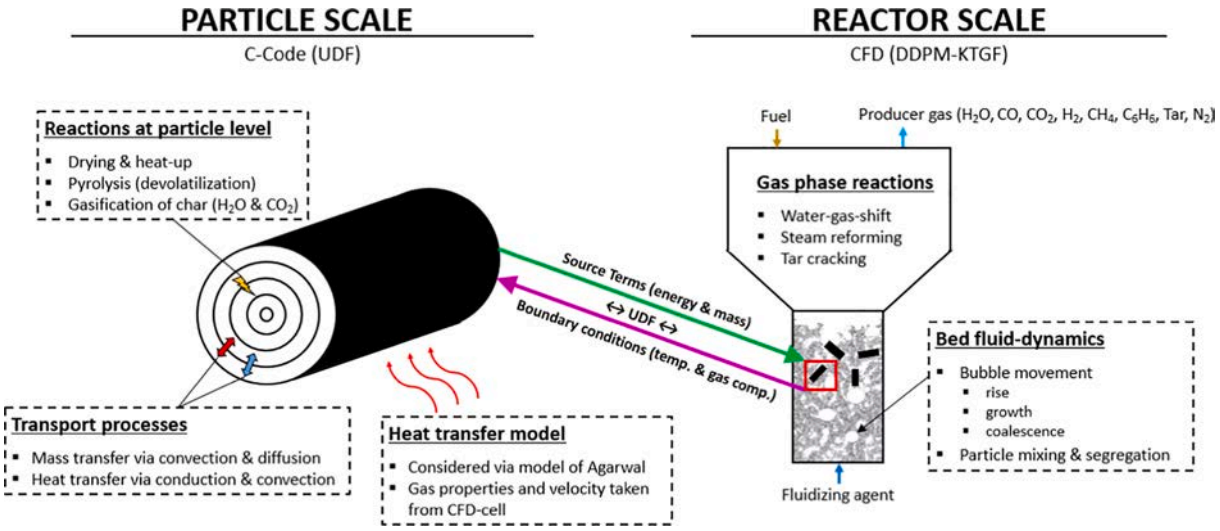

Fig. 1. Multi-scale methodology coupling the particle level and the reactor level via user-defined functions (UDF).

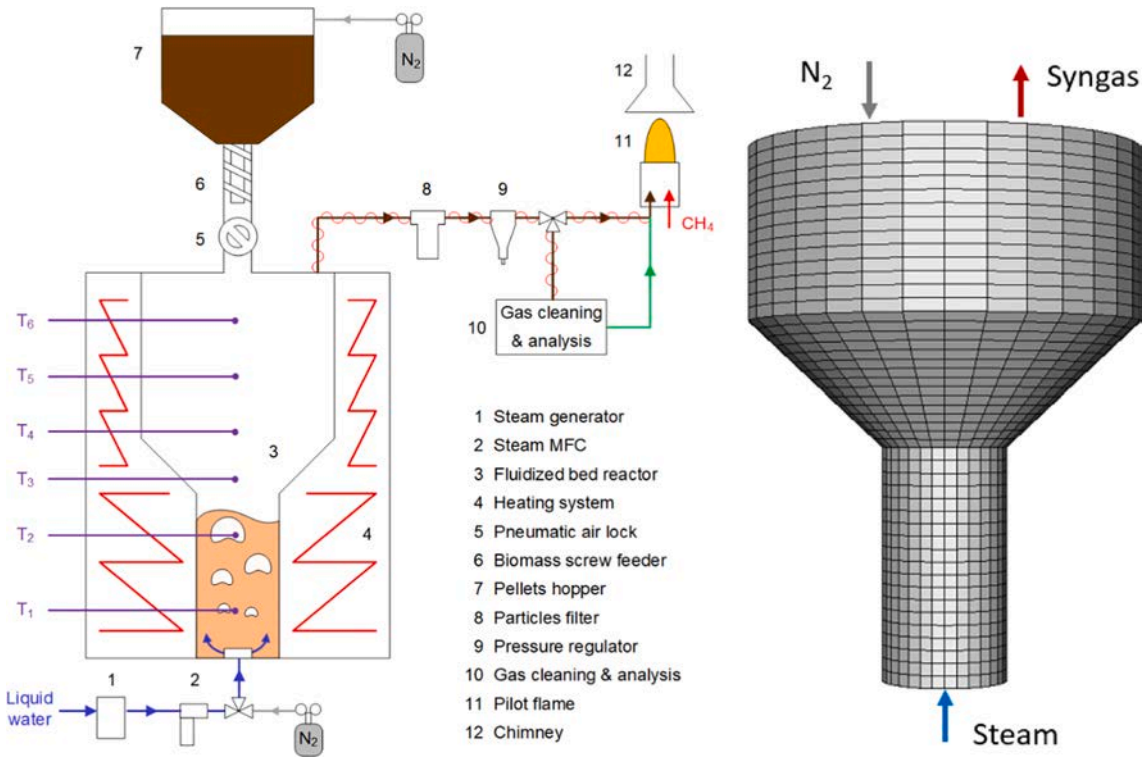

Fig. 2. Scheme of the experimental rig (left) and mesh of the bubbling fluidized bed gasifier (right).

CH_4, H_2 and O_2 are measured using an ABB AO2020 gas analysis. N_2 is calculated as the difference to 100%, as other gases are known to be only present in minor concentrations. Afterwards, the gas is burned in a pilot flame. A more detailed description of the experimental rig can be found in [49].

In order to obtain a well-defined experimental data-set, a measurement campaign was conducted during several days at the operation condition defined above. Very stable operation could be achieved and averaged measurement results together with their standard deviation were obtained for comparison with the simulation results.

3.2. Simulation setup

The mesh employed for the simulations was derived from the geometry of the fluidized bed rector which consists of a cylindrical bottom part of 80 mm diameter and 150 mm height. The bed is mainly located in this lower part of the reactor. Above, the reactor opens up in diameter from 80 to 250 mm in a conically-shaped part of 80 mm height followed by another cylindrical part of 110 mm height. This region is commonly referred to as freeboard. The geometry of the fluidized bed reactor was meshed using 4224 hexa cells and is shown in Fig. 2 on the right.

The simulation was set-up in ANSYS Fluent 2021 R2 as a transient simulation. A steady-state solution cannot be achieved due the constant particle movement in a fluidized bed. In order to obtain mean simulation results, time-dependent modelling data of a transient simulation needs to be averaged over a representative time period. A time-step of 0.0001 s (0.1 ms) was chosen for the fluid as well as for the solid time-step. The multiphase model was set to the DDPM employing the KTGF to calculate particle collisions. A primary phase representing the gas flow as well as a discrete phase representing the particles were defined. The discrete phase was set to granular whereas the chosen sub-models are given in Table 4. For more information and explanations on the description of the granular phase, please refer to the supplementary material.

Pretests of a cold-flow simulation were conducted in the framework of this study [32] to investigate the influence of turbulence which showed that the impact on the particle movement was rather small. This is in agreement with findings in literature [55–57] especially for cold-flow modelling. However, in this study, gas flow mixing and subsequent chemical reactions are of importance wherefore the influence of the turbulence plays a more important role and needs to be considered. Therefore, turbulence was modeled using the standard k-ε model which is commonly used in FBBG literature [58–61]. Enhanced wall treatment was activated and the turbulence multiphase model was set to dispersed due to the discrete character of the particles [11].

Table 4
Employed sub-models of the granular phase (see supplementary material for more information).

Granular property	Employed model
Multiphase model	DDPM
Particle interactions	KTGF
Turbulence model	Standard k-ε model (enhanced wall treatment)
Transition factor	0.65
Drag law	Gidaspow [31]
Granular viscosity	Syamlal and O'Brien [50]
Granular bulk viscosity	Lun et al. [51]
Solids pressure	Lun et al. [51]
Granular temperature	Algebraic
Frictional viscosity	Schaeffer [52]
Frictional pressure	Johnson and Jackson [53]
Friction packing limit	0.5
Angle of internal friction	30
Packing limit	0.52
Radial distribution function	Ma Ahmadi [54]
Specularity coefficient	0.5
Solid wall boundary condition	Johnson and Jackson [53]
Solid-solid restitution coefficient	0.8

3.3. Boundary conditions and initialization

The boundary conditions were set to represent the conditions of the experimental tests. A fixed temperature of 1200 K was set on the reactor walls according to the temperature measured in the oven surrounding

the gasifier. The temperature at the top wall was set to 1023 K as increased losses are expected due to reduced amount of insulation installed at this part of the gasifier. A no-slip boundary condition on the wall was set for the gas phase whereas a partial-slip condition was employed for the discrete phase according to Johnson and Jackson [53] using a specularity coefficient of 0.3 which is in the order of magnitude of 0.1 recommended for denser fluidization conditions [62]. The specularity coefficient is describing the effect of particle–wall friction and controls the momentum transfer from the particle to wall. A value of 0 represents a no-slip conditions whereas a value between 0 and 1 leads to a partial slip condition [62]. The boundary condition for the discrete phase was set to "reflect" for all surfaces including the syngas outlet, in order to prevent particles from leaving the domain. The preheated steam and nitrogen mixture entering at the bottom as well as the nitrogen flow were set according to experimental conditions.

As the model is set up as a transient simulation, an initial condition as close as possible to the stable operating condition of the gasifier needs to be defined in order to avoid long calculation times. Therefore, the initialization procedure as shown in Fig. 3 was developed. The reactor is filled with the bed material (red) at the very beginning followed by the injection of an initial fuel bed after one second of simulation time (blue). After this initialization routine, the fresh biomass fuel (green) is injected at a regular interval.

The bed material is injected in the reactor at the start of the simulation. In total 300.000 parcels represent 900 g of olivine, whereas each parcel depicts 110 olivine particles. This leads to a distinct reduction of calculation demand while still respecting the limit of cell size to parcel size ratio discussed in section 2.1.1. The simulation is then run for one second after a stable fluidization of the bed material is achieved. Afterwards, the initial bed of fuel particles at different states of conversion is injected in the freeboard of the reactor. The properties of each of the particles is calculated previously using the standalone version of the particle model. In contrast to the coupled calculations, the boundary conditions (e.g. temperature, gas velocity and gas composition) for the standalone particle model can only be set to a constant value for which average conditions in the bed were used. However, the results of the standalone model give a very good approximation of the initial fuel bed, since the variations in boundary conditions in a fluidized bed are limited. The data necessary as the initial condition for the coupled calculation is calculated for different states of conversion using the standalone particle model and later patched to the injected initial fuel particles via a user defined function. This includes the composition of the gas phase and the solid phase as well as the temperature in each control volume of the particle.

The number of fuel particles initially present in the reactor was estimated based on the fuel feeding rate. Based on a biomass feeding rate of 320 g/h and the biomass density of 1318 kg/m^3, a fresh fuel particle is fed to reactor every 7.5 s. Together with the assumption that char particles having a mass smaller than 0.5% of the initial mass are elutriated from the reactor, this leads to about 475 fuel particles in the reactor at stable operation conditions.

All of the initial fuel particles are treated similar as the fresh biomass, which is introduced to the reactor at a regular interval of 7.5 s corresponding to the fuel feeding rate of the experiments. The particle model is solved for all char and biomass particles after each fluid time-step and source terms for energy and species are updated accordingly. After about 10 s of process time, the gas composition at the outlet is getting constant. From there on, a further time-span of 20 s (Ostermeier et al. [63] recommended a time-span of 10 s when investigating just fluid-dynamics), was simulated to average the results of the simulation. The gas composition at the outlet, the pressure drop across the bed and the temperatures at the measurement points of the experimental setup along the reactor height are recorded. The initialization method developed allows for a very short period of only 30 s of process time compared to about 3600 s of process time that would be required if the process were modelled from the beginning and only fresh biomass particles were introduced to the reactor.

Due to the limitation of the maximal particle size in relation to the cell size of the CFD mesh, it was necessary to employ a "reverse clustering" (i.e. splitting) method for the fuel particles. The possibility to employ such an approach has been confirmed by ANSYS Fluent who also successfully used this method in the past [64]. The rather big particle size combined with the small reactor diameter in the case of the investigated lab-scale unit would require a very coarse mesh not suitable for application in CFD. Therefore, each fuel particle is represented by several parcels having only a fraction of the actual particle mass. Each particle was represented by 50 parcels, which leads to 23,750 fuel parcels in the gasifier. This ensures for each cell of the mesh to be able to contain at least 5 fuel parcels (while respecting the packing limit) and allows to maintain a parcel size sufficiently smaller than the cell size as suggested by ANSYS Fluent [65]. The particle model is solved for each parcel using the actual size of the particle whereas source terms were scaled accordingly. This reverse clustering approach leads to a comparably high calculation demand. However, when applying the coupled model for bigger facilities, this procedure is not necessary as the ratio of particle size to cell size will be larger. Moreover, the common clustering approach, where one parcel represents several fuel parcels, can be applied in such cases which further reduces the computational demand.

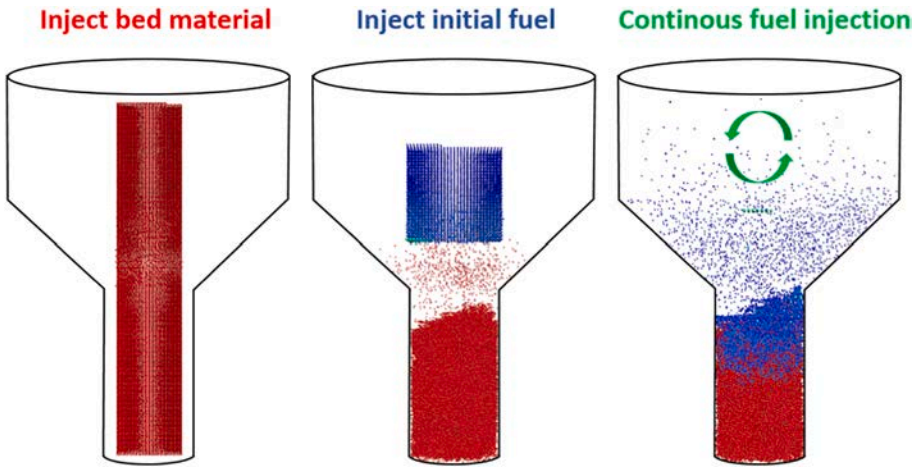

Fig. 3. Step-wise initialization of the particulate phase. Injection of the bed material (red) is followed by the injection of an initial fuel bed (blue) containing particles at different states of conversion, which is followed by a continuous supply of fresh biomass (green).

4. Results and discussion

First, results of the standalone particle model are presented. Different gasification kinetics are evaluated and compared with experimental data from literature. Furthermore, the full conversion of a fresh fuel particle including pyrolysis and gasification is analyzed in detail using the standalone model. Afterwards, the results of the coupled multi-scale model are presented and validated using experimental data generated in the framework of this study.

4.1. Results of the standalone particle model

In the following section, different char gasification kinetics are evaluated and results at the particle level calculated with the standalone version of the PM are presented.

4.1.1. Evaluation of gasification kinetics

A similar version of the standalone PM as used in this study was already validated for the case of fluidized bed pyrolysis [23], however, gasification has not been investigated in detail. Therefore, two different char gasification kinetics by Mermoud et al. [25] and Van de Steene et al. [26] were implemented in the existing model. The kinetics were validated using data of gasification experiments conducted by Reschmeier et al. [66]. Experiments of biomass pyrolysis in a fluidized bed by Reschmeier et al. [67] were already successfully modelled using the standalone PM while evaluating different heat transfer models for fluidized bed conditions by von Berg et al. in a previous publication [23]. In [66], Reschmeier et al. investigated gasification of char from softwood pellets in a small-scale bubbling fluidized reactor using steam as fluidization agent. The mass loss of several char particles during gasification at 850 °C was measured using a fluidized bed on a balance. To check if the model can predict this mass loss accurately, a simulation using the standalone particle model was set up considering the experimental conditions of Reschmeier. The experiments are based on char particles obtained from pyrolysis of softwood pellets, which is the same fuel employed for the experiments in the present study. To achieve a representative initial condition for the char particle, the simulation was started using properties of fresh softwood pellets. The modelling results show that after approximately one minute, pyrolysis is finished and the conditions of an initial char particle are reached. From there on, gasification is the main process of conversion. In Fig. 4, modelling results of the mass loss over time using the kinetics by Mermoud et al. [25] and Van de Steene et al. [26] are compared to experimental findings. The kinetics of Van de Steene predict a considerably faster conversion rate leading to a more than twice as fast char conversion when compared to the kinetics of Mermoud. Altogether, the faster kinetics of Van de Steene seem to match the experimental data better, especially when considering the time until conversion reaches 100%. Total particle conversion is reached after about 1600 s for the experimental test and after 1100 s and 2700 s when employing Van de Steene or Mermoud kinetics, respectively. Therefore, the kinetic model of Van de Steene will be used further on. Moreover, the current version of the PM does not consider particle attrition and fragmentation which are relevant in fluidized bed conditions and would also result in faster particle conversion. Therefore, the choice of the faster kinetic rate is more reasonable at the moment.

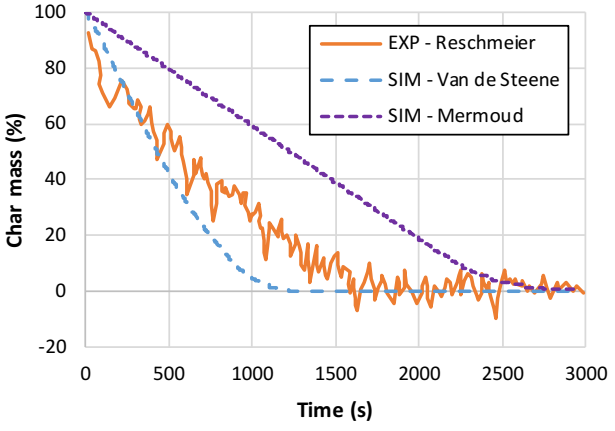

Fig. 4. Comparison of modelling and experimental results for the mass loss of a char particle (obtained from pyrolysis of a 6 mm cylindrical softwood pellet) during steam gasification in a bubbling fluidized bed at 1173 K. Experimental data taken from Reschmeier et al. [66].

4.1.2. Results at the particle level

The standalone model was used to evaluate and visualize the conversion of a fuel particle. The coupled multi-scale model is run only for a short time when compared to the time needed for the total conversion of a fresh fuel particle and would therefore not allow to show the total conversion process of a fuel particle. The standalone particle model was used employing same settings as in the coupled simulations, however, a constant temperature of 1073 K and a constant gas composition were set for the standalone calculations. The results of the model show that in general, the particle conversion can be divided into a pyrolysis and a gasification step. These two steps can be assumed to occur sequentially as gasification shows very slow kinetics compared to the fast pyrolysis. The evolution of devolatilization during pyrolysis is shown in Fig. 5. The evolution of temperature, moisture, fresh biomass and char is plotted over timer for every second control volume (CV) in the particle whereas CV 1 is the innermost and CV 10 the outermost CV. The temperature in every CV is rising with increasing time, whereas the heat-up in the outer part is significantly faster due to the rather low thermal conductivity of

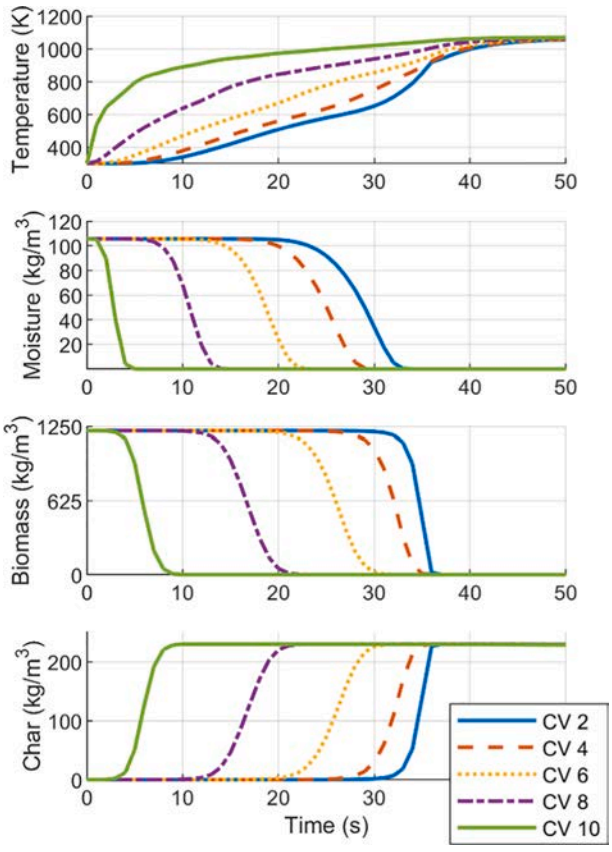

Fig. 5. Intra particle gradients during pyrolysis for temperature, moisture, biomass and char amount in the individual control volumes (CV 1: centre, CV 10: surface) for cylindrical softwood pellets with 6 mm diameter and 18 mm length. The boundary conditions were set according to the experiments conducted in this study.

the biomass. It takes about 50 s until the temperature in the whole particle has reached the surrounding temperature and is almost evenly distributed. The evolution of the moisture content shows quick drying in the CV at the surface (less than 5 s) whereas above 30 s are necessary to remove all moisture in the central CV in order to achieve total drying of the particle. The evolution of char proceeds in the opposite way to that of biomass, as char is produced during the pyrolysis of the fresh biomass. It takes about 40 s until all biomass is converted to char, whereas distinct gradients are visible for the different solid species. The trend of the moisture and biomass curve suggests that drying might be limiting the pyrolysis reaction. Bryden et al. [68] also found a significant effect of moisture content on the pyrolysis time for thermally thick particles. During pyrolysis, almost 80% of the initial particle mass is devolatilized.

The char produced during pyrolysis is then gasified. The evolution of temperature and the amount of char during the gasification of the particle is shown in Fig. 6.a for every second CV. The temperature shows an almost homogeneous distribution with slightly lower temperatures in the center of the particle for the whole time of the gasification period which takes about 4000 s. The temperature diffrence between the CV at the center and the surface of the particle is at maximum 15 K. The evolution of residual char during gasification shows that gradients of solid char inside the particle are present, however they are much more subtle compared to the gradients present during pyrolysis. When running the same simulation at a higher temperature of 1173 K still within the typical operating range of FBBG [5,69], the model predicts distinct gradients also during gasification as shown in Fig. 6.b. In this case, the outer layer of the particle is already fully gasified after 75% of the time needed for total conversion (about 1100 s) and temperature gradients of about 40 K are predicted. Furthermore, particle gradients during gasification will be even more distinct when bigger fuel particles are employed.

The evolution of fuel conversion is visualized in Fig. 7 for the case at 1073 K. During the first 40 s shown in the upper row of the figure, the changes inside the particle lead to clearly visible gradients until the whole fresh biomass is converted to char. Afterwards, the residual char is gasified considering H_2O and CO_2 as gasification agents. The gradual fade from black to white over time represents the consumption of char. Simultaneously, the particle diameter is reduced due to particle shrinkage considered in the model. During pyrolysis, shrinkage occurs beginning from the surface of the particle simultanously with the devolatilization in each CV and proceeds into the center until the whole particle is converted into char. During gasification, a homogeneous shrinkage over the whole particle radius can be observed while the residual char is gasified.

4.2. Results of the multi-scale model

In the following section, the results of the coupled simulations are discussed and validated using experimental data. Therefore, the measurement and modelling results of pressure drop, temperature at different positions in the reactor as well as the gas composition at the reactor outlet are compared. Furthermore, the modelling results at the particle level are investigated in more detail demonstrating the possibilities and advantages of the employed multi-scale approach.

4.2.1. Comparison with experimental data

In Fig. 8, the modelling results (blue) are compared with experimental data (orange). The obtained modelling results of time dependent pressure drop over the bed presented in Fig. 8.a show a fluctuating behavior typical for a bubbling fluidized bed. For easier comparison, the mean pressure drop averaged over the sampling time of 20 s marked in the diagram is plotted (solid blue line) together with the standard deviation (dashed blue line). When compared to the mean experimental pressure drop (solid orange line) and its standard deviation (dashed orange line), the model shows acceptable, but not particularly good agreement with the measurement results. The average value of the

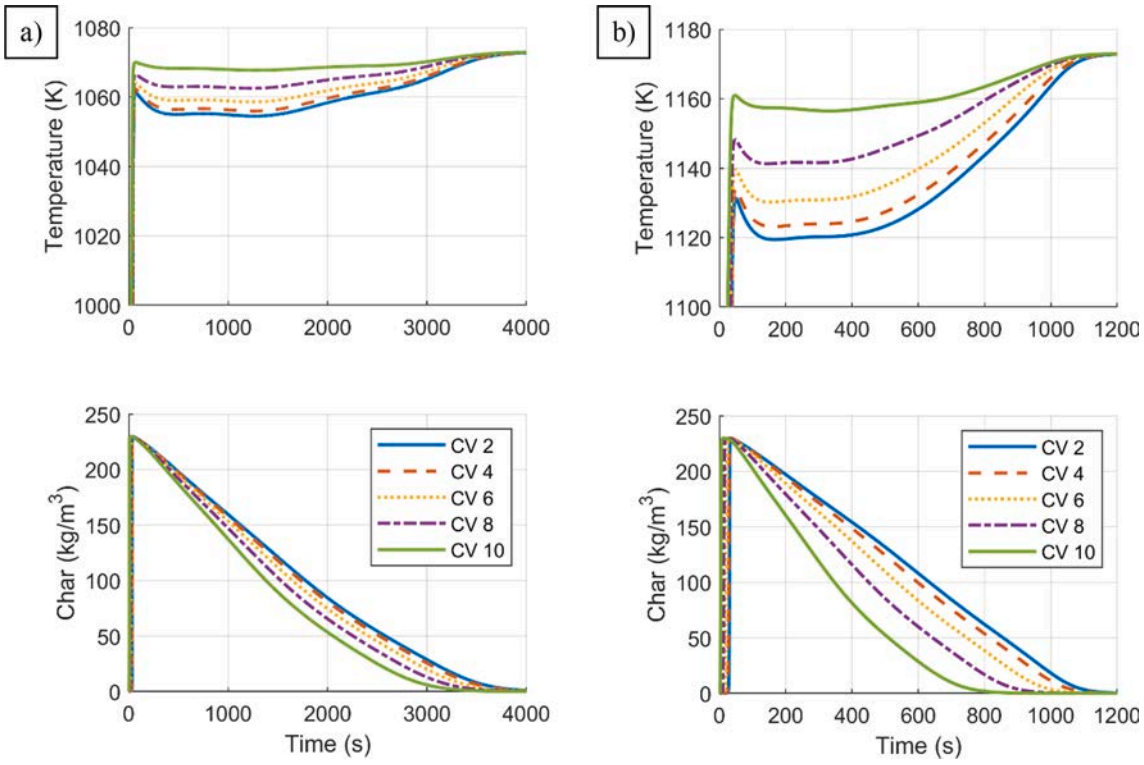

Fig. 6. Intra particle gradients during char gasification for temperature and char amount (the char particle was obtained via pyrolysis of a cylindrical softwood pellets with 6 mm diameter and 18 mm length). a) employing an operating temperature of 1073 K (same as in the experiments and coupled simulations) shows less pronounced gradients, b) employing a temperature of 1173 K leads to more distinct gradients. All other boundary conditions were set according to the experiments conducted in this study. (CV 1: centre, CV 10: surface).

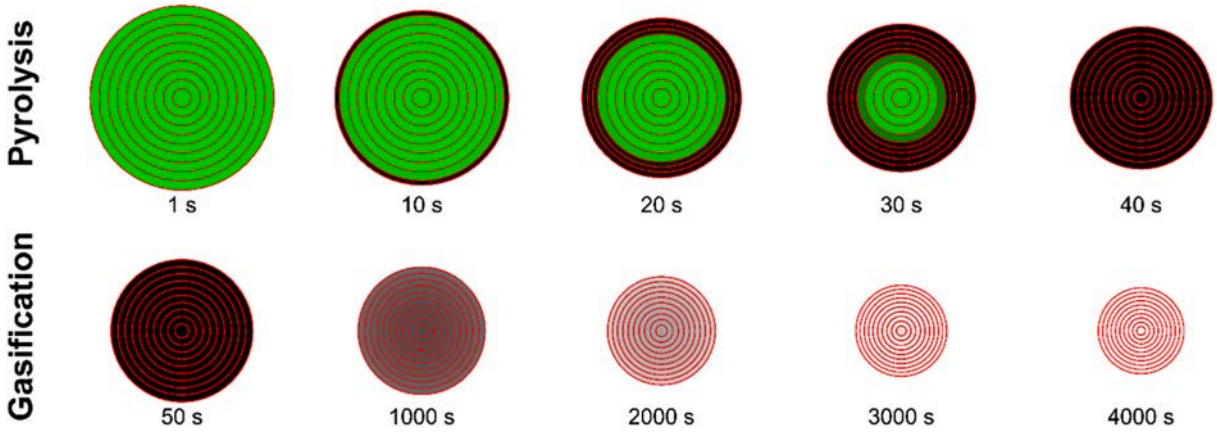

Fig. 7. Fuel conversion during pyrolysis and gasification at different states of conversion (green: fresh biomass, black: char, white: ash).

experiments is about 1268 ± 75 Pa whereas the modelling results lead to 904 ± 308 Pa, showing a deviation of about 29%. The disk-shaped marker shows the time of the initial injection of the fuel whereas the diamond-shaped markers indicate the continuous fuel feeding every 7.5 s. Fig. 8.b shows the mean temperature at the different heights inside the reactor. The same sampling period as defined in Fig. 8.a was used to calculate the average temperature of the simulation results. The experimental data shows a homogeneous temperature distribution inside the bed with almost the same temperature at T1 and T2. The freeboard is about 50 to 100 K warmer showing the highest temperature at T4. A similar trend can be seen for the modelling results, although the temperature increase in the freeboard is significantly lower. However, it must be emphasized that radiation, which could have a non-negligible influence under the conditions studied, is only considered for the particle level and not at the reactor level for the sake of simplicity. The standard deviation of both modelling and experimental results in the bed is very small, which can be explained by the thermal inertia of the bed material. Both experimental and modelling results show the highest standard deviation at T3, which is located just above the bed. This might be explained by the energy demand needed for drying and pyrolysis of fresh fuel particles which are likely to be located at the top of the bed depending on the intensity of fluidization. Fig. 8.c shows the comparison of dry gas composition. Overall, good agreement can be seen for all components. However, there is a deviation for CO, CO_2 and H_2 which seems to be connected to the water–gas-shift reaction. This deviation can probably be diminished by employing different WGS kinetics available in literature but shall not be further investigated in the current study. The highest deviation is present for N_2 which can be partly explained by the fact that the experimental result of N_2 is not measured but calculated as the difference to 100% and therefore all the measurement errors of the other gas components are accumulated.

Comparison of the measured and modelled fuel mass inside the reactor can give a good indication if the model can describe the overall processes inside the reactor. During the experiments, the total mass of fuel particles in the bed was measured to be around 0.024 kg. Even after different hours of operation, no significant change of the total mass could be seen. This can be attributed to the rather low ash content of the employed fuel of 0.3 mass % in dry basis combined with the overall low fuel feeding rate which leads to about 0.001 kg/h of ash fed to the reactor. Moreover, elutriation of very small particles and dust was observed during the experimental tests. The evolution of the total fuel mass over time predicted by the model is shown in Fig. 9 (right axis, green curve). The magenta markers show the initial fuel injection (disk-shaped) and the continuous fuel feeding (diamond-shaped). When a new fuel particle is fed to the reactor every 7.5 s, the mass increases instantaneously. In between the feeding cycles, the overall mass declines due to conversion of the individual fuel particles. The mass decrease due to conversion in between injections is about the same as the mass introduced into the reactor at each injection, which ensures that the overall fuel mass in the reactor stays almost constant during continuous operation. In average, the model predicts a total fuel mass of about 0.025 kg showing a deviation of below 5% and therefore acceptable agreement with the measured value.

The intensity of mixing between bed and fuel particles and the resulting segregation effects can be described as defined by Goldschmidt et al. [70]. In the present study, the degree of segregation was defined as the ratio of the mean height of the fuel particles to the mean height of the bed particles. Therefore, it shows a value of 1 for perfectly mixed fuel and bed particles and a value above 1 if the fuel particles show a greater mean particle height than the bed particles. The evolution of the simulated degree of segregation is shown in in Fig. 9 (left axis, blue curve). At the moment of the initial fuel injection, the degree of segregation is way above 1 as the fuel particles are injected in the freeboard. Afterwards, the particles fall onto the top of the bed and are slowly mixed with the bed material. During the investigated time span of 30 s, the segregation did not lead to a constant value indicating that the mixing and segregation processes did not reach an equilibrium. It seems like a constant value of about 1.2 is reached after about 30 s indicating that a great number of fuel particles is floating on top of the inert bed material. This is in well accordance with literature were a flotsam behavior of the low density biomass and char particles is commonly assumed [71,72]. However, the focus of the current study is on the multi-scale coupling approach and therefore does not further investigate this phenomenon.

In the coupled simulation, the particle model is solved for every fuel parcel in the reactor according to its local boundary conditions. The evolution of mean temperature and density for every fresh biomass parcel injected to the reactor during the simulation is plotted over its residence time in Fig. 10. The initial injection consists of 23,750 parcels whereof most of them are partly converted to char. However, only the data of the 50 fresh biomass parcels is shown here (disk-shaped marker). Every 7.5 s, a new particle is injected represented by 50 parcels each (diamond-shaped marker). A similar evolution for both temperature and density can be seen for all parcels of a injection showing slight deviations due to the small changes in boundary conditions.

The trajectory of a single parcel is visualized in Fig. 11, showing the x- and y-position of the parcel plotted over its residence time as it moves through the reactor. The mean position of the parcel is visualized by a white circle including the standard deviation. Fig. 11.a shows the trajectory of a fresh biomass parcel with a density of about 1318 kg/m^3. After the fresh fuel particle is injected into the freeboard (diamond-shaped marker), it falls onto the top of the bed and is mainly located in this area. As the surface of the fluidized bed is constantly changing due to the constant particle movement, an average bed height is calculated during the sampling period and marked by the black dotted line. Most of

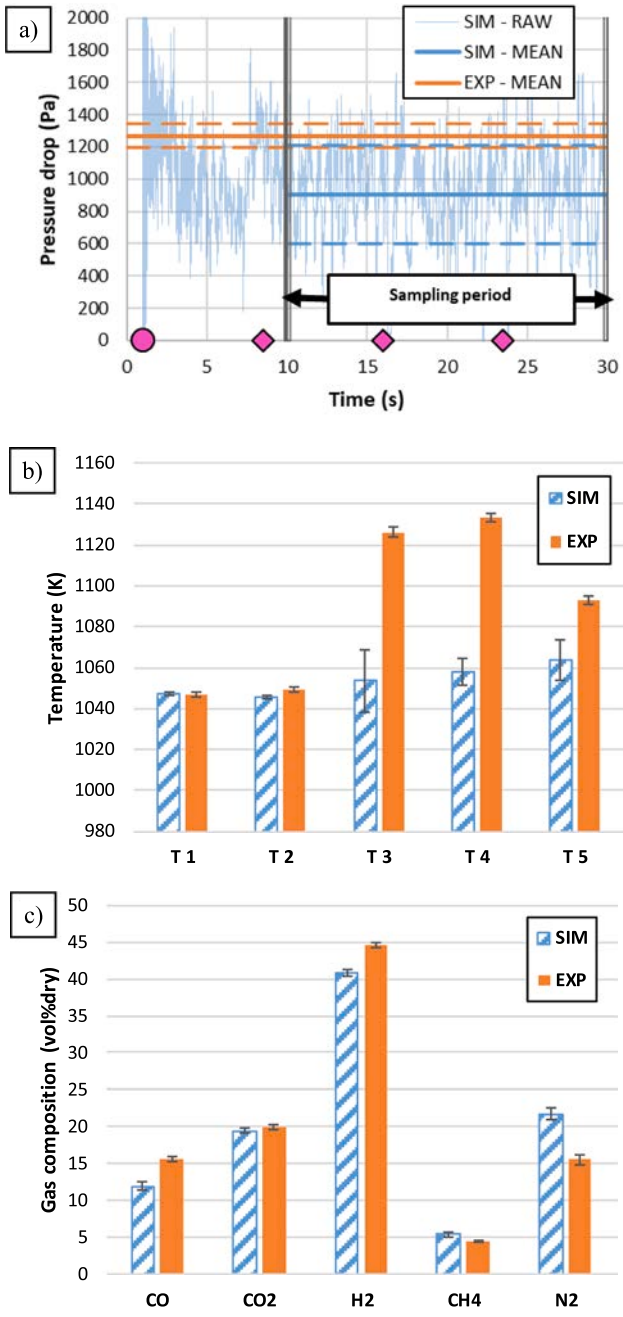

Fig. 8. Comparison of modelling results (blue) and experimental data (orange): a) pressure drop over the fluidized bed shown as time-dependent data as well as mean values (the dashed line shows the standard deviation), b) temperature along the reactor height, c) dry gas composition at the reactor outlet.

the time, the parcel is located close to this area meaning it is mostly located at the bed surface. Due to the eruption of bubbles on the surface of the bed, the parcel is thrown into the freeboard from time to time. An intensive mixing of fuel and bed particles cannot be observed in the investigated case. Findings from the experimental tests also suggested that the low-density fuel and char particles tend to be located in the upper part of the bed when removing the fuel and bed material from the reactor. In Fig. 11.b, the trajectory of an almost fully converted char parcel with a density of about 150 kg/m^3 is shown. When compared to the heavy fresh biomass particle which penetrates deeper into the bed from time to time, the lighter char particle spends most of the time in the freeboard or at the surface of the bed.

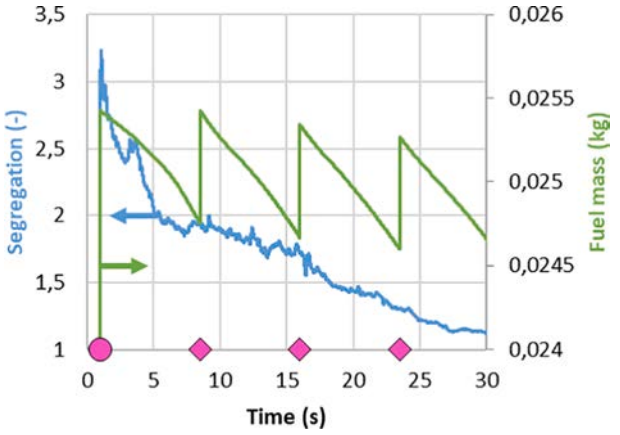

Fig. 9. Evolution of total fuel mass in the reactor (right axis, green) and particle segregation (left axis, blue). Magenta markers indicate injection of fuel.

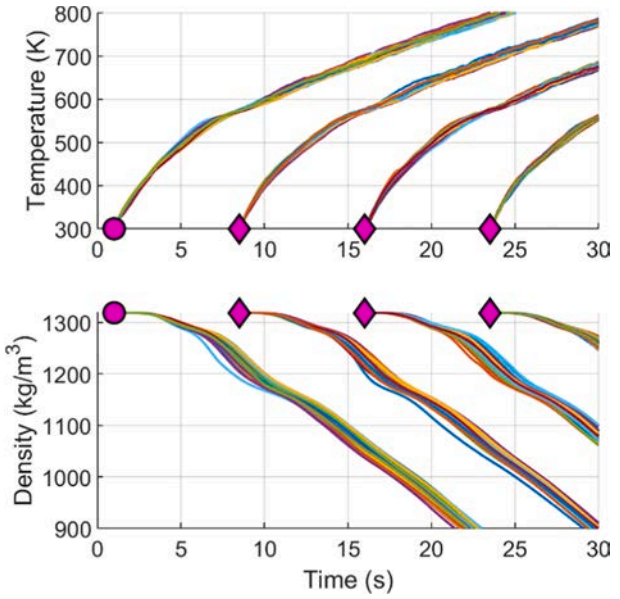

Fig. 10. Fuel parcel temperature and density over residence time.

4.2.2. *Calculation time*

The simulations were conducted on a Windows 10 workstation equipped with an Intel® Core™ i7-8700 K CPU @ 3.7 GHz and 64 GB RAM. ANSYS Fluent 2021 R2 was run using 4 cores in parallel. It was observed that the choice of the parallelization method was essential to achieve a significant speed-up when running in parallel. When using the default method employed by Fluent (called 'metis'), the calculation time did not improve significantly. This parallelization method splits the reactor horizontally. Therefore, the computational load of the PM is not evenly distributed on all cores when running in parallel as most fuel particles will be located in the same partition due to their flotsam behavior. However, a significant reduction of calculation time was achieved when employing the partitioning method called 'cylindrical theta-coordinate' which lead to a much better load distribution over all cores. Overall, the PM showed to be well suited for parallelization when distributing the computational load evenly over all cores. In our case, the coupled-model showed better parallelization potential than estimated from our previous study investigating modelling fluidized bed reactors using the DDPM at cold-flow conditions [32]. Future modelling studies at larger scale will benefit from these findings and use an increased number of cores.

Altogether, one time-step of 0.0001 s took about 3 s calculation time

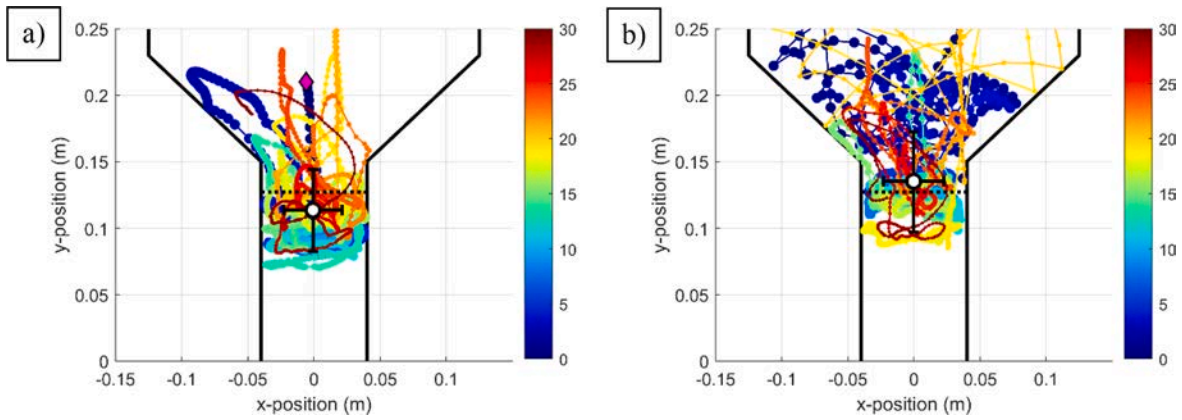

Fig. 11. Representative trajectories of parcels at different states of conversion in the reactor coloured by residence time: a) fresh fuel (high density) and b) almost fully converted char particle (low density). The black dotted line represents the average bed height.

including the solution of the PM and the solution of the DDPM for all parcels which leads to a calculation time of about 8 h per second and therefore about ten days for a time-span of 30 s. In the current study, employing the number of bed and fuel particles as shown in Table 5, the solution of the PM for reacting fuel parcels accounts for about 44% of the total calculation time. In this case, each reacting fuel particle was represented by 50 parcels due to the limitation of the DDPM, which consequently leads to a fiftyfold increase of the time needed for the solution of the PM when compared to the case where the PM is solved for every fuel particle only. However, even under these disadvantageous conditions, the overall calculation time is still manageable. If the parcel size was not limited by the small geometry of the lab-scale reactor, each fuel particle could be represented by one parcel. This would allow to reduce the share in calculation time for the PM from 44% to about 2% as shown in Table 5 (Current study mod.). Furthermore, the overall calculation time would thereby be reduced to about 57% of the calculation time needed in the current study.

When analyzing the estimated calculation time for larger applications, there are two main potentials which can lead to a further reduction of the calculation time needed for the PM as shown in Table 5. First, a large geometry would probably allow for a regular clustering of fuel particles meaning one parcel would represent several fuel particles for which the PM is only solved once. Second, larger biomass plants usually operate at a lower mass fraction of reacting particles compared to the current study [73]. In summary, it seems like the PM developed in this study can be applied for even large plants with only a relatively small contribution to the overall calculation time. Therefore, if it is feasible to model a reactor with the DDPM, it could probably also be modeled with the coupled CFD-PM approach with an expected estimated increase of computation time of less than 2%.

5. Conclusions

In the present study, we have shown for the first time that it is feasible to incorporate a detailed 1D particle model into a commercial CFD software for modeling fluidized bed biomass gasification. The multi-scale approach allows for a detailed analysis of particle movement including mixing and segregation at the reactor level while at the same time facilitates a comprehensive description at the particle level. The current study employs the model for fluidized bed biomass gasification, however, the approach can easily be adapted for almost any different fluidized bed application where the particle level needs to resolved in

Table 5
Representation of fuel and bed material particles for the current study and potentials for reducing the calculation time of the particle model (PM).

			DDPM		PM
			Bed material	Fuel	
Current study	Mass at constant operation (approx.)	g	900	25	
	Mass fraction	%	97.3	2.7	
	Number of particles (approx.)	-	33,000,000	475	
	Number of particles / parcel	-	110	1 / 50 = 0.02	
	Number of parcels	-	300,000	23,750	
	Percentage of calculation time	%	56		44
Current study mod.	Number of particles / parcel	-	110	1 (↑)	
	Number of parcels	-	300,000	475	
	Percentage of calculation time	%	98		2
Large scale	Number of particles / parcel	-	110	> 1 (↑)	
	Representative mass fraction	%	99.5	0.5 (↓)	
	Percentage of calculation time	%	≥ 98		< 2

detail e.g. for chemical looping, reduction of iron oxide or combustion. The validation study conducted in this work showed good agreement between simulation results and experimental data of temperature as well as producer gas composition. However, the pressure drop was significantly underestimated by the model in the current case and needs to be further investigated in future work e.g. via using a different drag model. Moreover, an in-depth view at the conversion of individual particles along their trajectory through the reactor was given.

The current study showed that the time needed to solve the coupled model was feasible for a lab-scale reactor. By using an initialization method whereby an initial fuel bed consisting of particles of varying grade of conversion is injected, an initial condition close to the operating point of the reactor was achieved allowing for short calculation times. Furthermore, we could show that the share of time needed to solve the particle model could be further reduced in larger applications as the limitation of the DDPM regarding the fuel parcel size will drop and the mass fraction of reacting particles will be smaller. Therefore, we estimated that the increase of calculation time will probably be less than 2 % compared to an uncoupled solution of the DDPM. As the DDPM is in general well suited for modelling larger applications, the developed approach should be applicable in larger facilities with a rather limited increase in total calculation time.

With the developed multi-scale modelling approach, we present a powerful tool allowing detailed modelling of a reacting particle inside a fluidized bed respecting intra-particle gradients. Further investigation is planned employing the approach for a pilot plant fluidized bed biomass gasification reactor. Moreover, future work shall focus on a more detailed mechanism for tar formation and cracking as tar contamination is still one of the main problems hindering the application of fluidized bed biomass gasification in a larger scale. The simplified reaction mechanisms of pyrolysis and tar cracking currently used form the foundation for easy implementation of more detailed chemistry in further work.

CRediT authorship contribution statement

Lukas von Berg: Conceptualization, Methodology, Software, Formal analysis, Investigation, Data curation, Writing – original draft. **Andrés Anca-Couce:** Methodology, Conceptualization, Supervision, Funding acquisition, Writing – review & editing. **Christoph Hochenauer:** Project administration, Supervision. **Robert Scharler:** Methodology, Conceptualization, Supervision, Funding acquisition, Writing – review & editing.

Declaration of Competing Interest

The authors declare that they have no known competing financial interests or personal relationships that could have appeared to influence the work reported in this paper.

Acknowledgements

This project has received funding from European Union's Horizon 2020 Research and Innovation Programme under grant agreement number 731101 (BRISK II). Furthermore, the financial support of the COMET Module project BIO-LOOP (Austrian Research Promotion Agency – FFG - Project Number 872189) funded by the federal government of Austria and the federal province Styria is gratefully acknowledged. The authors want to thank Mario Blehrmühlhuber for conducting cold-flow simulations and evaluating the applicability of the DDPM for the developed model. We further want to thank Markus Braun for his helpful hints when using the DDPM and Simon Schneiderbauer for his advice regarding the coupling strategy.

Appendix A. Supplementary data

Supplementary data to this article can be found online at https://doi.org/10.1016/j.fuel.2022.124677.

References

[1] Masson-Delmotte V, Zhai P, Pirani A, Connors SL, Péan C, Berger S, et al. Summary for Policymakers. Sixth Assessment Report of the Intergovernmental Panel on Climate Change (IPCC). 2021.
[2] Anca-Couce A, Hochenauer C, Scharler R. Bioenergy technologies, uses, market and future trends with Austria as a case study. Renew Sustain Energy Rev 2021;135:110237. https://doi.org/10.1016/j.rser.2020.110237.
[3] Molino A, Chianese S, Musmarra D. Biomass gasification technology: The state of the art overview. J Energy Chem 2016;25:10–25. https://doi.org/10.1016/j.jechem.2015.11.005.
[4] Gómez-Barea A, Ollero P, Leckner B. Optimization of char and tar conversion in fluidized bed biomass gasifiers. Fuel 2013;103:42–52. https://doi.org/10.1016/j.fuel.2011.04.042.
[5] Gómez-Barea A, Leckner B. Modeling of biomass gasification in fluidized bed. Prog Energy Combust Sci 2010;36:444–509. https://doi.org/10.1016/j.pecs.2009.12.002.
[6] Adamczyk WP. Application of the Numerical Techniques for Modelling Fluidization Process Within Industrial Scale Boilers. Arch Comput Methods Eng 2017;24:669–702. https://doi.org/10.1007/s11831-016-9186-z.
[7] Ding J, Gidaspow D. A bubbling fluidization model using kinetic theory of granular flow. AIChE J 1990;36:523–38. https://doi.org/10.1002/aic.690360404.
[8] Cundall PA, Strack ODL. A discrete numerical model for granular assemblies. Géotechnique 1979;29:47–65. https://doi.org/10.1680/geot.1979.29.1.47.
[9] Andrews MJ, O'Rourke PJ. The multiphase particle-in-cell (MP-PIC) method for dense particulate flows. Int J Multiph Flow 1996;22:379–402. https://doi.org/10.1016/0301-9322(95)00072-0.
[10] Snider DM. An Incompressible Three-Dimensional Multiphase Particle-in-Cell Model for Dense Particle Flows. J Comput Phys 2001;170:523–49. https://doi.org/10.1006/jcph.2001.6747.
[11] ANSYS Fluent. Theory Guide 2021 R2 2021.
[12] Alobaid F, Almohammed N, Massoudi Farid M, May J, Rößger P, Richter A, et al. Progress in CFD Simulations of Fluidized Beds for Chemical and Energy Process Engineering. Prog Energy Combust Sci 2022;91:100930.
[13] Cloete S, Amini S. The dense discrete phase model for simulation of bubbling fluidized beds: Validation and verification. ICMF-2016 – 9th International Conference on Multiphase Flow. 2016.
[14] Adnan M, Sun J, Ahmad N, Wei JJ. Comparative CFD modeling of a bubbling bed using a Eulerian-Eulerian two-fluid model (TFM) and a Eulerian-Lagrangian dense discrete phase model (DDPM). Powder Technol 2021;383:418–42. https://doi.org/10.1016/j.powtec.2021.01.063.
[15] Schneiderbauer S, Kinaci ME, Hauzenberger F. Computational Fluid Dynamics Simulation of Iron Ore Reduction in Industrial-Scale Fluidized Beds. Steel Research International 2020. https://doi.org/10.1002/srin.202000232.
[16] Li C, Eri Q. Comparison between two Eulerian-Lagrangian methods: CFD-DEM and MPPIC on the biomass gasification in a fluidized bed. Biomass Convers Biorefinery 2021. https://doi.org/10.1007/s13399-021-01384-2.
[17] Ostermeier P, Fischer F, Fendt S, DeYoung S, Spliethoff H. Coarse-grained CFD-DEM simulation of biomass gasification in a fluidized bed reactor. Fuel 2019;255:115790. https://doi.org/10.1016/j.fuel.2019.115790.
[18] Wang H, Zhong Z. A mixing behavior study of biomass particles and sands in fluidized bed based on CFD-DEM simulation. Energies 2019;12(9):1801.
[19] Yang S, Wang H, Wei Y, Hu J, Chew JW. Particle-scale modeling of biomass gasification in the three-dimensional bubbling fluidized bed. Energy Convers Manag 2019;196:1–17. https://doi.org/10.1016/J.ENCONMAN.2019.05.105.
[20] Gupta S, Choudhary S, Kumar S, De S. Large eddy simulation of biomass gasification in a bubbling fluidized bed based on the multiphase particle-in-cell method. Renew Energy 2021;163:1455–66. https://doi.org/10.1016/j.renene.2020.07.127.
[21] Kong D, Luo K, Wang S, Yu J, Fan J. Particle behaviours of biomass gasification in a bubbling fluidized bed. Chem Eng J 2022;428:131847. https://doi.org/10.1016/j.cej.2021.131847.
[22] Yang M, Zhang J, Zhong S, Li T, Løvås T, Fatehi H, et al. CFD modeling of biomass combustion and gasification in fluidized bed reactors using a distribution kernel method. Combust Flame 2022;236:111744.
[23] von Berg L, Soria-Verdugo A, Hochenauer C, Scharler R, Anca-Couce A. Evaluation of heat transfer models at various fluidization velocities for biomass pyrolysis conducted in a bubbling fluidized bed. Int J Heat Mass Transf 2020;160:120175. https://doi.org/10.1016/j.ijheatmasstransfer.2020.120175.
[24] Dupont C, Boissonnet G, Seiler JM, Gauthier P, Schweich D. Study about the kinetic processes of biomass steam gasification. Fuel 2007;86:32–40. https://doi.org/10.1016/j.fuel.2006.06.011.
[25] Mermoud F, Golfier F, Salvador S, Van De Steene L, Dirion JL. Experimental and numerical study of steam gasification of a single charcoal particle. Combust Flame 2006;145:59–79. https://doi.org/10.1016/j.combustflame.2005.12.004.
[26] Van de steene L, Tagutchou JP, Escudero Sanz FJ, Salvador S. Gasification of woodchip particles: Experimental and numerical study of char-H2O, char-CO2, and char-O2 reactions. Chem Eng Sci 2011;66(20):4499–509.

[27] Bates RB, Ghoniem AF, Jablonski WS, Carpenter DL, Altantzis C, Garg A, et al. Steam-air blown bubbling fluidized bed biomass gasification (BFBBG): Multi-scale models and experimental validation. AIChE J 2017;63(5):1543–65.
[28] Baruah D, Baruah DC. Modeling of biomass gasification: A review. Renew Sustain Energy Rev 2014;39:806–15. https://doi.org/10.1016/j.rser.2014.07.129.
[29] Safarian S, Unnþórsson R, Richter C. A review of biomass gasification modelling. Renew Sustain Energy Rev 2019;110:378–91. https://doi.org/10.1016/J.RSER.2019.05.003.
[30] Anca-Couce A, Zobel N. Numerical analysis of a biomass pyrolysis particle model: Solution method optimized for the coupling to reactor models. Fuel 2012;97:80–8. https://doi.org/10.1016/J.FUEL.2012.02.033.
[31] Gidaspow D, Bezburuah R, Ding J. Hydrodynamics of circulating fluidized beds: Kinetic theory approach. Proc 7th Eng Found Conf Fluid 1992.
[32] Blehrmühlhuber M. CFD Simulation of Hydrodynamics in Fluidized Beds. Master Thesis, TUG 2018.
[33] Shadle L, Guenther C, Cocco R, Panday R. NETL Challenge Problem III (2010): NETL's Circulating Fluidized Bed (CFB). and PSRI's Bubbling Fluid Bed (BFB). 2010.
[34] Tricomi L, Melchiori T, Chiaramonti D, Boulet M, Lavoie JM. Numerical investigation of a cold bubbling bed throughout a dense discrete phase model with KTGF collisional closure. Biofuels Eng 2018;2:32–50. https://doi.org/10.1515/bfuel-2017-0003.
[35] Peng Z, Doroodchi E, Luo C, Moghtaderi B. Influence of void fraction calculation on fidelity of CFD-DEM simulation of gas-solid bubbling fluidized beds. AIChE J 2014;60:2000–18. https://doi.org/10.1002/aic.14421.
[36] Wang FY, Bhatia SK. A generalised dynamic model for char particle gasification with structure evolution and peripheral fragmentation. Chem Eng Sci 2001;56:3683–97. https://doi.org/10.1016/S0009-2509(01)00060-4.
[37] ANSYS Fluent. Users Guide 2021 R2 2021.
[38] Biba V, Macák J, Klose E, Malecha J. Mathematical Model for the Gasification of Coal under Pressure. Ind Eng Chem Process Des Dev 1978;17:92–8. https://doi.org/10.1021/i260065a017.
[39] Hou K, Hughes R. The kinetics of methane steam reforming over a Ni/α-Al2O catalyst. Chem Eng J 2001;82:311–28. https://doi.org/10.1016/S1385-8947(00)00367-3.
[40] Van den Aarsen FG. Fluidised bed wood gasifier performance and modeling. Enschede (Netherlands): Technische Hogeschool Twente; 1985.
[41] Scharler R, Gruber T, Ehrenhöfer A, Kelz J, Bardar RM, Bauer T, et al. Transient CFD simulation of wood log combustion in stoves. Renew Energy 2020;145:651–62.
[42] Anca-Couce A, Sommersacher P, Scharler R. Online experiments and modelling with a detailed reaction scheme of single particle biomass pyrolysis. J Anal Appl Pyrolysis 2017;127:411–25. https://doi.org/10.1016/j.jaap.2017.07.008.
[43] Mellin P, Kantarelis E, Yang W. Computational fluid dynamics modeling of biomass fast pyrolysis in a fluidized bed reactor, using a comprehensive chemistry scheme. Fuel 2014;117:704–15. https://doi.org/10.1016/J.FUEL.2013.09.009.
[44] Anca-Couce A, Caposciutti G, Gruber T, Kelz J, Bauer T, Hochenauer C, et al. Single large wood log conversion in a stove: Experiments and modelling. Renew Energy 2019;143:890–7.
[45] Ranzi E, Cuoci A, Faravelli T, Frassoldati A, Migliavacca G, Pierucci S, et al. Chemical kinetics of biomass pyrolysis. Energy Fuels 2008;22(6):4292–300.
[46] Agarwal PK. Transport phenomena in multi-particle systems—IV. Heat transfer to a large freely moving particle in gas fluidized bed of smaller particles. Chem Eng Sci 1991;46:1115–27. https://doi.org/10.1016/0009-2509(91)85104-6.
[47] Hayhurst AN, Parmar MS. Measurement of the mass transfer coefficient and sherwood number for carbon spheres burning in a bubbling fluidized bed. Combust Flame 2002;130:361–75. https://doi.org/10.1016/S0010-2180(02)00387-5.
[48] Bates RB, Altantzis C, Ghoniem AF. Modeling of Biomass Char Gasification, Combustion, and Attrition Kinetics in Fluidized Beds. Energy Fuels 2016;30:360–76. https://doi.org/10.1021/acs.energyfuels.5b02120.
[49] von Berg L, Pongratz G, Pilatov A, Almuina-Villar H, Hochenauer C, Scharler R, et al. Correlations between tar content and permanent gases as well as reactor temperature in a lab-scale fluidized bed biomass gasifier applying different feedstock and operating conditions. Fuel 2021;305:121531.
[50] Syamlal M, Rogers W, O'Brien TJ. MFIX documentation theory guide n.d. https://doi.org/10.2172/10145548.
[51] Lun CKK, Savage SB, Jeffrey DJ, Chepurniy N. Kinetic theories for granular flow: inelastic particles in Couette flow and slightly inelastic particles in a general flowfield. J Fluid Mech 1984;140:223–56. https://doi.org/10.1017/S0022112084000586.
[52] Schaeffer DG. Instability in the evolution equations describing incompressible granular flow. J Differ Equ 1987;66:19–50. https://doi.org/10.1016/0022-0396(87)90038-6.
[53] Johnson PC, Jackson R. Frictional–collisional constitutive relations for granular materials, with application to plane shearing. J Fluid Mech 1987;176:67–93. https://doi.org/10.1017/S0022112087000570.
[54] Ahmadi G, Ma D. A thermodynamical formulation for dispersed multiphase turbulent flows—1: Basic theory. Int J Multiph Flow 1990;16:323–40. https://doi.org/10.1016/0301-9322(90)90062-N.
[55] Adnan M, Sun J, Ahmad N, Wei JJ. Multiscale modeling of bubbling fluidized bed reactors using a hybrid Eulerian-Lagrangian dense discrete phase approach. Powder Technol 2020;376:296–319. https://doi.org/10.1016/j.powtec.2020.07.111.
[56] Lungu M, Wang H, Wang J, Yang Y, Chen F. Two-fluid model simulations of the national energy technology laboratory bubbling fluidized bed challenge problem. Ind Eng Chem Res 2016;55:5063–77. https://doi.org/10.1021/acs.iecr.5b04511.
[57] Li T, Dietiker JF, Shahnam M. MFIX simulation of NETL/PSRI challenge problem of circulating fluidized bed. Chem Eng Sci 2012;84:746–60. https://doi.org/10.1016/j.ces.2012.09.024.
[58] Qi T, Lei T, Yan B, Chen G, Li Z, Fatehi H, et al. Biomass steam gasification in bubbling fluidized bed for higher-H2 syngas: CFD simulation with coarse grain model. Int J Hydrogen Energy 2019;44(13):6448–60.
[59] Wang S, Luo K, Hu C, Sun L, Fan J. Impact of operating parameters on biomass gasification in a fluidized bed reactor: An Eulerian-Lagrangian approach. Powder Technol 2018;333:304–16. https://doi.org/10.1016/j.powtec.2018.04.027.
[60] Ansarifar H, Shams M. Numerical simulation of hydrogen production by gasification of large biomass particles in high temperature fluidized bed reactor. Int J Hydrogen Energy 2018;43:5314–30. https://doi.org/10.1016/j.ijhydene.2017.10.132.
[61] Ku X, Jin H, Lin J. Comparison of gasification performances between raw and torrefied biomasses in an air-blown fluidized-bed gasifier. Chem Eng Sci 2017;168:235–49. https://doi.org/10.1016/j.ces.2017.04.050.
[62] Cloete JH, Cloete S, Radl S, Amini S. Evaluation of wall friction models for riser flow. Powder Technol 2016;303:156–67. https://doi.org/10.1016/j.powtec.2016.07.009.
[63] Ostermeier P, DeYoung S, Vandersickel A, Gleis S, Spliethoff H. Comprehensive investigation and comparison of TFM, DenseDPM and CFD-DEM for dense fluidized beds. Chem Eng Sci 2019;196:291–309. https://doi.org/10.1016/j.ces.2018.11.007.
[64] Personal contact with ANSYS Fluent. 2021.
[65] Multiphase Modeling using ANSYS Fluent - Discrete Phase Model (DPM) 2015.
[66] Reschmeier R, Karl J. Experimental study of wood char gasification kinetics in fluidized beds. Biomass Bioenergy 2016;85:288–99. https://doi.org/10.1016/J.BIOMBIOE.2015.05.029.
[67] Reschmeier R, Roveda D, Müller D, Karl J. Pyrolysis kinetics of wood pellets in fluidized beds. J Anal Appl Pyrolysis 2014;108:117–29. https://doi.org/10.1016/j.jaap.2014.05.009.
[68] Bryden KM, Hagge MJ. Modeling the combined impact of moisture and char shrinkage on the pyrolysis of a biomass particle. Fuel 2003;82:1633–44. https://doi.org/10.1016/S0016-2361(03)00108-X.
[69] Karl J, Pröll T. Steam gasification of biomass in dual fluidized bed gasifiers: A review. Renew Sustain Energy Rev 2018;98:64–78. https://doi.org/10.1016/j.rser.2018.09.010.
[70] Goldschmidt MJV, Link JM, Mellema S, Kuipers JAM. Digital image analysis measurements of bed expansion and segregation dynamics in dense gas-fluidised beds. Powder Technol 2003;138:135–59. https://doi.org/10.1016/j.powtec.2003.09.003.
[71] Soria-Verdugo A, Garcia-Gutierrez LM, Sanchez-Delgado S, Ruiz-Rivas U. Circulation of an object immersed in a bubbling fluidized bed. Chem Eng Sci 2011;66:78–87. https://doi.org/10.1016/j.ces.2010.10.006.
[72] Soria-Verdugo A, Garcia-Gutierrez LM, García-Hernando N, Ruiz-Rivas U. Buoyancy effects on objects moving in a bubbling fluidized bed. Chem Eng Sci 2011;66:2833–41. https://doi.org/10.1016/j.ces.2011.03.055.
[73] Gómez-Barea A, Nikolopoulos A. Doctoral Course: CFD modelling of fluidized bed reactors using ANSYS-FLUENT. Chemical and Environmental Engineering Department: University of Seville; 2018.